EUROPEAN ORGANIZATION FOR NUCLEAR RESEARCH
CERN-AB DEPARTMENT

CERN-AB-2004-012 (ABP)

GSI-Acc-Note-2004-02-001
LBNL-54594
SLAC-PUB-10350

CAN LOW ENERGY ELECTRONS AFFECT HIGH ENERGY PHYSICS ACCELERATORS?

R. Cimino[1,2], I.R. Collins[2], M.A. Furman[3], M. Pivi[4], F. Ruggiero[2], G.Rumolo[5], F. Zimmermann[2]

The properties of the electrons participating in the build up of an electron cloud (EC) inside the beam-pipe have become an increasingly important issue for present and future accelerators whose performance may be limited by this effect. The EC formation and evolution are determined by the wall-surface properties of the accelerator vacuum chamber. Thus, the accurate modeling of these surface properties is an indispensible input to simulation codes aimed at the correct prediction of build-up thresholds, electron-induced instability or EC heat load. In this letter, we present the results of surface measurements performed on a prototype of the beam screen adopted for the Large Hadron Collider (LHC), which presently is under construction at CERN. We have measured the total secondary electron yield (SEY) as well as the related energy distribution curves (EDC) of the secondary electrons as a function of incident electron energy. Attention has been paid, for the first time in this context, to the probability at which low-energy electrons ($\leq$ 20 eV) impacting on the wall create secondaries or are elastically reflected. It is shown that the ratio of reflected to true-secondary electrons increases for decreasing energy and that the SEY approaches unity in the limit of zero primary electron energy.
PACS numbers: 79.20.Hx ; 29.27.Bd; 41.75.Lx

Submitted to Physical Review Letters

1) LNF-INFN, Frascati, Italy; 2) CERN, Geneva, Switzerland; 3) LBNL, Berkeley, USA; 4) SLAC, Stanford, USA; 5) GSI, Darmstadt, Germany

Geneva, Switzerland

AB/DEP/Reps

11 February, 2004

Can low energy electrons affect high energy physics accelerators?

R. Cimino[a,b], I.R. Collins[b], M.A. Furman[c], M. Pivi[d], F. Ruggiero[b], G. Rumolo[e], and F. Zimmermann[b]
a) LNF-INFN, Frascati, Italy; b) CERN, Geneva, Switzerland; c) LBNL, Berkeley, USA; d) SLAC, Stanford, USA; e) GSI, Darmstadt, Germany
(Dated: February 9, 2004)

The properties of the electrons participating in the build up of an electron cloud (EC) inside the beam-pipe have become an increasingly important issue for present and future accelerators whose performance may be limited by this effect. The EC formation and evolution are determined by the wall-surface properties of the accelerator vacuum chamber. Thus, the accurate modeling of these surface properties is an indispensible input to simulation codes aimed at the correct prediction of build-up thresholds, electron-induced instability or EC heat load. In this letter, we present the results of surface measurements performed on a prototype of the beam screen adopted for the Large Hadron Collider (LHC), which presently is under construction at CERN. We have measured the total secondary electron yield (SEY) as well as the related energy distribution curves (EDC) of the secondary electrons as a function of incident electron energy. Attention has been paid, for the first time in this context, to the probability at which low-energy electrons ($\lesssim$ 20 eV) impacting on the wall create secondaries or are elastically reflected. It is shown that the ratio of reflected to true-secondary electrons increases for decreasing energy and that the SEY approaches unity in the limit of zero primary electron energy.

PACS numbers: 79.20.Hx ; 29.27.Bd; 41.75.Lx

In 1989 an instability driven by photoelectrons was observed at the KEK Photon Factory (PF). It was not until 1994 that its origin was correctly identified as due to the formation of an electron cloud [1, 2]. Since then several proton-storage rings (PSR [3, 4], SPS, PS), electron-positron colliders [4] (PEP-II, KEKB, BEPC, DAFNE) and synchrotron radiation (SR) sources when operating with positrons (APS) have reported similar beam instabilities and other related detrimental effects, which are now understood to be due to a coupling between the beam and an EC in the vacuum chamber that contains the beam. These effects, usually referred to as electron-cloud effects, include beam-induced electron multipacting (BIEM), observed at the ISR as early as 1977 when operated with bunched proton beams [5]. A more distant related effect is the two-stream instability which affects unbunched, coasting, proton beams [6]. Deleterious effects of the EC include interference with diagnostic devices, coupled-bunch coherent beam instabilities, and/or single-bunch incoherent effects such as emittance increase. In general, the EC is significant in machines that make use of intense, closely-spaced, short, positively-charged bunches, and vacuum chambers of relatively small transverse dimensions, such as the positron damping rings of future linear colliders. In the cases of the B factories PEP-II and KEKB, the EC in the positron rings led to important operational limitations of the initial designs, and to an intense search for, and implementation of, mitigating mechanisms [4, 7, 8].

BIEM can be qualitatively explained as follows: a bunch in the beam may generate one or a few "seed" electrons, *e.g.*, by ionization of the residual gas or by photoemission, which are then accelerated by the bunch electric field in the direction perpendicular to the beam motion. If the bunch charge and the bunch spacing satisfy a certain condition, the traversal time of the electron across the vacuum chamber equals the time interval between successive bunches, and a resonance condition is thereby established. If, in addition, the effective secondary electron yield (SEY) at the chamber is larger than unity, which is a likely condition in many cases, as it was at the ISR, the electron population grows rapidly in time with successive bunch passages, leading to a high electron density, and, hence, to detrimental effects such as a rapid vacuum pressure rise resulting in beam loss. A closely related phenomenon, called trailing-edge multipacting, has also been observed for a single proton bunch at the PSR when the beam intensity exceeds a certain threshold [9]. It could prove important for other existing or planned spallation neutron sources, like SNS or ESS. The ECs observed at all above-mentioned machines (except for the ISR, PSR and, possibly, PEP-II) are not ordinarily dominated by resonant effects like BIEM, owing to the operational choices for bunch spacing and intensity. Nevertheless, the chamber geometry and beam parameters are such as to lead to an electron density large enough to cause undesirable effects. In the case of positron storage rings, and for the LHC [10, 11], the EC is mainly seeded by photoelectrons emitted off the chamber walls by the synchrotron radiation (SR) [12] produced by the beam as it traverses the bending magnets in the ring. For the other hadron machines, the seed mechanism is typically ionization of residual gas and/or electron generation by stray beam particles striking the chamber walls at grazing angles. In almost all cases, however, the secondary emission process is the crucial ingredient in amplifying the energy and the intensity of the electrons of the EC.

A novel EC effect is expected at the LHC, namely an excess power deposition on the vacuum chamber beam screen due to the EC bombardment. Since the LHC magnets are superconducting, being operated at 1.9 K, it is important to understand and control the heat load

on the cryogenic system. To protect the cold bore (vacuum envelope) from SR irradiation and image currents, a beam screen (BS) will be inserted. The BS will be held at a temperature between 5 and 20 K. The available BS cooling capacity is exceeded if the EC-induced heat load surpasses 1 to 1.5 W/m [14] in any of the two rings, and in this case, the EC will limit the achievable machine performance. During the past several years the EC has been studied experimentally at several machines including the two B factories, BEPC, APS, PSR, PS, SPS and RHIC by means of dedicated instruments and computer simulations such as POSINST, ECE and ECLOUD (see Ref. [4] for details). These simulations, which take as input the secondary emission yield as a function of the energy E_0 of the incident electron, $\delta(E_0)$, and the energy distribution of the emitted secondaries, $d\delta/dE(E_0)$, among other ingredients, have had some notable successes in modeling many aspects of the EC, including single- and multi-bunch instabilities for positron rings with short bunches, and trailing-edge multipacting in the PSR [6] so that a reasonable degree of confidence now exists in the predictions of these codes and in the understanding of the EC that has thereby been obtained. However, the simulations have until now been limited also by uncertainties in the measurements of the SEY at low incident-electron energy ($E_0 \lesssim 20$ eV). In this letter it is shown that, in order to correctly predict any EC induced additional heat load in the LHC, it is essential to determine accurately the energy distribution of the emitted secondary electrons, $d\delta/dE$, and the relative composition of the emitted secondary electrons *i.e.* the relative ratio of backscattered to true secondaries. The SEY for actual LHC beam screen samples, measured down to unprecedentedly low energies and here presented, shows that, as the incident electron energy E_0 is lowered below ~ 10 eV, the SEY does not decrease monotonically, as previously assumed [4], but rather shows an unexpected upturn, leading to a high value of the SEY at zero energy, namely $\delta(0) \sim 1$. The importance of studying the properties of low-energy primary electrons interacting with the industrially prepared sample is underscored by the notion that, according to simulations, when an EC develops, the energy distribution of the electrons impinging on the wall peaks at very low energy ($\lesssim 20$ eV) [13]. The data here presented are fed into the aforementioned computer simulations codes.

The simulations confirm the importance of the very low-energy electrons for correctly estimating EC effects and for addressing the operational reliability of future machines like the LHC, the GSI-SIS, the SNS, or linear-collider damping rings. The EDC at low primary energy was analyzed by a dedicated experimental apparatus, presently at CERN, which is described in detail elsewhere [15]. In brief, a combination of a cryo-pump and a UHV μ-metal chamber reduces residual magnetic field near the sample, and allows operation in a vacuum better than 10^{-10} Torr without bake-out. The EDC were collected by a Spectaleed Omicron Retarding Field Analyser (RFA), specially modified to be able to collect angle-integrated EDCs at very low impinging electron energy. The e^- beam was always smaller than 1 mm^2 in transverse cross-sectional area and stable (both in current and position) for energies between 30 and 350 eV, as confirmed by a line profile and by stability tests done using a home-made 1 mm slot Faraday cup. The sample could be kept at a constant temperature between 8 and 400 K. A bias voltage was applied, in order to measure secondary emission for very low primary electron energies, while keeping the gun in a region where it was stable and focused. The samples studied were all part of the real chamber surface in the LHC. We find it reasonable to assume that the surfaces of other technical materials used for vacuum chambers exhibit the same general behaviour as the data presented here. Testing this assumption calls for more systematic and broader investigations of the type described in this article. Figure 1 shows a sub-

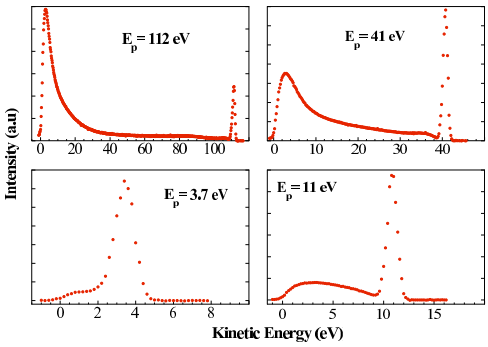

FIG. 1: Measured energy distribution curves (EDC) of a fully scrubbed Cu surface at about 10 K for different primary electron energies at normal incidence.

set of EDC's taken as a function of primary energy from an as-received Cu sample at 10 K after it was conditioned by bombarding with more than 1 C/cm^2 of 400 eV e^- in an open geometry. This e^- dosing, known as scrubbing [4], will not be addressed in this letter, but it is known to produce surface modifications vs. dosing up to a stable surface (i.e., a surface with a SEY that no longer changes with further electron dosing). From the spectra in Fig. 1, it is clear that at primary energies higher than 100 eV the main contribution to the EDC is given by the secondary electrons emitted with 0 to 15 eV kinetic energy and only a small fraction is due to electrons elastically reflected from the surface. As the primary energy gets lower, the ratio between reflected and secondary electrons increases, until reflection becomes dominant for primary energies below 20 eV. From the available data it is possible by simple numerical integration, to extract the ratio between *true secondary* and *elastically reflected* electrons for each primary energy. In this letter, we do not consider *rediffused* electrons (sometimes referred to in literature), since at low primary energy the separation between true secondaries and rediffused electrons becomes rather arbitrary. We then consider all the electrons emitted be-

tween 0 eV up to the onset of the clear elastic peak at the primary electron energy as true secondary electrons, while the integral under this peak gives the amount of elastically reflected electrons. In Fig. 2 we present SEY

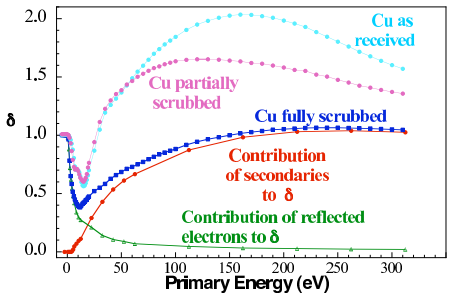

FIG. 2: Total SEY (δ) at normal incidence and the contribution of secondary and reflected electrons from a fully scrubbed Cu surface at about 10 K as a function of E_0.

measurements of the same sample as used for measuring the EDC, taken before, during, and after scrubbing. First, the curves show that the behaviour at low primary energies is largely independent of $\delta_{\max}$ and of the degree of scrubbing. From the EDC data of Fig. 1 and the fully scrubbed SEY curve of Fig. 2 we can determine the yield of reflected electrons per incident primary electron. This is shown as a fit and decomposition in Fig. 2, for the case of the fully scrubbed surface. At low energy most of the impinging electrons are reflected by the Cu surface, resulting in a SEY value that approaches unity in the limit of vanishing primary energy. The value of the observed SEY minimum and the corresponding energy depend on the actual sample and on its conditions (temperature, scrubbing etc.), while the overall shape of the SEY curve is preserved and a SEY value close to unity has been measured at low E_0 in all cases. The data demonstrate the importance of the reflected electrons at low primary energy and suggest, for the first time in this context, that low energy electrons may have long survival time inside the accelerator vacuum chambers due to their high reflectivity. This notion may explain why in the KEK B factory [4] and in the CERN SPS [16] a memory effect has been observed, namely, the EC build up observed during the passage of a bunch train is enhanced by the passage of a preceding bunch train, even if the time interval between the two trains is quite long (500 ns in the SPS and 1μs at KEKB).

The EC simulation codes have been described in detail elsewhere [4]. To simulate LHC, the two main sources of electrons are given by photoemission from SR and by secondary emission from electrons hitting the walls. The photo-electrons are modelled by macroparticles, each of which represents a certain large number of real electrons, carrying a fixed charge. The secondary electron emission mechanism either adds to these a variable number of macroparticles (POSINST) or changes the charges of the existing macroparticles and splits them if necessary (ECLOUD), according to the SEY model outlined below.

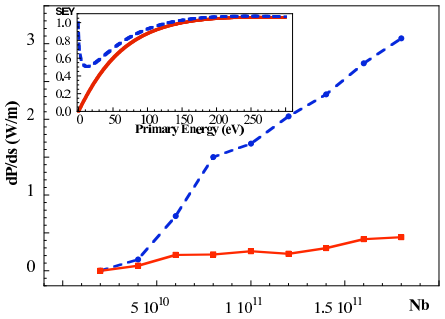

FIG. 3: Simulated average heat load in an LHC dipole magnet as function of proton bunch population at 0.5 TeV, calculated by extrapolating the best fit to the data of fig. 2 (shown in the insert) for a SEY with $\delta^*_{\max} = 1.7$ and $E_{\max} = 240$ eV, considering the elastic reflection (dashed line) or ignoring it (full line)

The SEY for perpendicular incidence at a primary energy E_0 is described as the sum of two components, SEY $= \delta_{\rm el} + \delta_{\rm true}$, each of which is approximated by fits to measurements [4]. The true secondary component is $\delta_{\rm true}(x) = \delta^*_{\max} sx/(s-1+x^s)$, where $x = E/E^*_{\max}$ and where the value $s \approx 1.35$ has been obtained from several measured data sets [17]. There are only two free parameters, namely the energy at which the true yield is maximum, $E^*_{\max}$, and the effective maximum secondary emission yield $\delta^*_{\max}$. The measurements of elastic reflection reported in this letter are very well parametrized by $\delta_{\rm el}(E) = (\sqrt{E} - \sqrt{E+\epsilon_0})^2/(\sqrt{E} + \sqrt{E+\epsilon_0})^2$, with only one fit parameter ϵ_0. The above formula for $\delta_{\rm el}$ can be obtained from a simple quantum-mechanical model [19], considering a plane-wave electron wave function incident on a negative potential step of depth ϵ_0. The expression for $\delta_{\rm el}$ introduces a minimum in the total SEY curve, as it is seen in Fig. 2. It always yields a reflectivity of 1 in the limit that E approaches 0 eV, consistent with the measurements presented above.

We remark that previously used parametrizations either ignored the elastic component, or used a phenomenological formula for δ_{el} [4, 7, 17] obtained by simple extrapolation down to $E_0 = 0$, of available data which were taken with higher incident electron energy E_0 than those discussed here. Although the results of such simulations [18] did show a substantial increase of the EC power deposition relative to those in which δ_{el} was wholly neglected, the amount of such an increase was generally different than what is presented in this article, and the details of the mechanism were not well understood.

SEY parametrizations, with and without elastic reflection are shown for an energy range between 0 and 300 eV in the insert of Fig. 3. The model with elastic reflection is the best fit to the data (Fig. 2) of the fully scrubbed surface with ($\delta^*_{\max} = 1.06$ and $E_{\max} = 262$

eV.) We have used such fit to extrapolate, according to the above equations, SEY curves with different values of $\delta^*_{\rm max}$ and $E_{\rm max}$ eV, using them as input to simulations, modelling the behavior of an LHC beam, consisting of 72 bunches with 25 ns spacing through an arc dipole chamber. Heat loads, simulated as a function of bunch intensity, are shown in Fig. 3 for a true secondary maximum yield of $\delta^*_{\rm max} = 1.7$. Such value of $\delta^*_{\rm max}$ is expected during the intermediate stages of the scrubbing process. It is clear that it is important to correctly model the

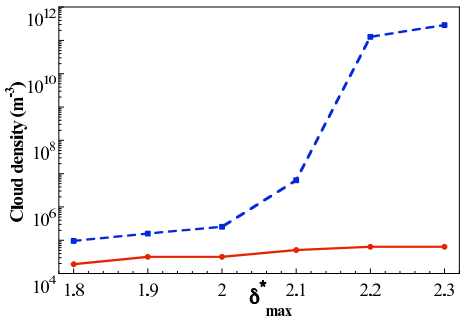

FIG. 4: Simulated average EC density in a field-free section of the GSI-SIS18 as a function of δ_{max}, comparing the cases with (dashed line) and without (full line) elastic reflection.

SEY at low energy. In fact, without considering reflected low energy electrons (full line), the simulated heat load is well within the available cooling budget in all calculated cases, but this is no longer true if we include in the calculation the high reflectivity of low energy electrons, as reported in this paper. This specific result suggests the need of particular care in the LHC commissioning scenario. To present a second example, we now discuss the case of the synchrotron SIS18 at GSI, which will be upgraded so as to become an injector for the planned synchrotron SIS100. One of the possible operation scenarios presently foreseen requires the acceleration in the SIS18 of 4×10^{10} U^{73+} (packed in four 80 ns long bunches with a 100 ns spacing) to 1 GeV/u. Fig. 4 shows that the modeling of elastic reflection based on our data lowers the $\delta^*_{\rm max}$ threshold for the onset of the electron cloud to $\sim$ 2.2, whereas no significant EC is to be expected for $\delta^*_{\rm max}$ values beyond 2.3 without elastic reflection. Instability simulations have shown that the EC saturation densities for $\delta^*_{\rm max} \sim 2.2$ are sufficient to drive the beam unstable. The implications of the new parametrization here proposed for low energy electron SEY is currently under study for other present and planned accelerators. In conclusion, the experimental data and the simulations clearly demonstrate the importance of elastic electron reflection at low energies, whose probability is shown, in this study, to approach unity in the limit of zero incident energy. The data indicate that low-energy electrons are long-lived in the accelerator vacuum chamber, explaining the puzzling observations of memory effects seen at the KEK B factory and at the CERN SPS. Calculations including the measured elastic reflection predict a significantly higher heat load for the LHC arcs than previously expected and a possible EC formation in the heavy ion synchrotron SIS18 at GSI when upgraded to deliver the required currents for the future facilities. The results presented here, therefore, call for a general re-examination of EC predictions for all present and future accelerators, including linear-collider damping rings.

Acknowledgement. The authors are indebted to V. Baglin, G. Bellodi, M. Blaskiewicz, D. Schulte, and P. Strubin. This work was partially supported by INFN-group V and by the US DOE under contracts DE-AC03-76SF00515 and DE-AC03-76SF00098.

[1] M. Izawa, Y. Sato, and T. Toyomasu, Phys. Rev. Lett. 74, 5044 (1995).
[2] K. Ohmi, Phys. Rev. Lett. 75, 1526 (1995).
[3] M. Blaskiewicz, M.A. Furman, M. Pivi, R. J. Macek Phys. Rev. ST AB **6**, 014203, 2003; and ref. therein.
[4] Proc. ECLOUD'02, Geneva, April, 2002, CERN Yellow Report CERN-2002-001 (2002); and ref. therein.
[5] O. Gröbner, 10th Int. Conf. High Energy Accelerators, Protvino (1977).
[6] Proc. Workshop on: "Instabilities in High-Intensity Hadron Beams in Rings", Upton NY, AIP Conf. Proc. 496 (1999).
[7] Proc. Int. Workshop on Multibunch Instabilities in Future Electron and Positron Accelerators (MBI'97), Y.H. Chin (ed.), Tsukuba, KEK Proc. 97-17 (1997).
[8] Proc. Two-Stream Instabilities in Particle Accelerators and Storage Rings, Tsukuba, (2001).
[9] D. Neuffer, NIM A 321, p. 1 (1992).
[10] LHC Study Group, "The Large Hadron Collider – Conceptual Design," CERN/AC/95-05 (1995).
[11] F. Zimmermann, CERN-LHC-Project-Report-95 (1997).
[12] R. Cimino, I.R. Collins, V. Baglin, PRST AB 2, 063201 (1999).
[13] F. Zimmermann, Proc. Chamonix XI, CERN-SL-2001-003 DI (2001).
[14] U. Wagner, Proc. Chamonix XIII, to be published (2004).
[15] R. Cimino, I.R. Collins, Proc. 8th EVC, Berlin (2003).
[16] J.M. Jimenez et al., CERN LHC-P.R. 632 (2003).
[17] M. A. Furman and M. T. F. Pivi, PRST AB 5, 124404 (2003).
[18] M. A. Furman, LBNL-41482/CBP Note 247/LHC P. R. 180, (1998).
[19] M. Blaskiewicz, private communication (2003).